Granular core phenomenon induced by convection in a vertically vibrated cylindrical container

Jing Sun,[1] Chuanping Liu,[1,2] Ping Wu,[3,*] Zi-Ang Xie,[3] Kaiwei Hu,[1] and Li Wang[1,2]
[1]*School of Energy and Environment Engineering, University of Science and Technology Beijing, Beijing 100083, China*
[2]*Beijing Engineering Research Centre of Energy Saving and Environmental Protection, Beijing 100083, China*
[3]*School of Mathematics and Physics, University of Science and Technology Beijing, Beijing 100083, China*
(Received 24 June 2016; published 12 September 2016)

A mixture of 13X molecular sieve (13XMS) particles and glass particles with identical diameters is placed in a cylindrical container. Under vertical vibration, heavier glass particles tend to cluster and are wrapped inside the convection of 13XMS particles, resulting in the granular core phenomenon. The vibration frequency f strongly influences particle convection and particle cluster modes. By contrast, the effect of the dimensionless acceleration amplitude Γ can be neglected. For different f ranges, the granular core is classified as center-type and ring-type cores. For the center-type core, heavy particles are distributed as an approximate zeroth-order Bessel function of the first kind in the radial direction and an exponential function in the height direction. For the ring-type core, the concentration of heavy particles follows the power-series function in the radial direction. A granular transport model is then established based on heavy-particle movements under steady state to analyze the effect of vibration parameters and granular convection on density segregation.

DOI: 10.1103/PhysRevE.94.032906

I. INTRODUCTION

Granular materials, which comprise discrete solid particles, exhibit unique types of behavior, such as particle segregation [1–6], convection [7–13], and clustering [14–16], when externally excited. This phenomenon is due to the dissipation of kinetic energy during inelastic collision [17,18]. The granular segregation behavior of two or more kinds of particles under vertical vibration has been widely studied but is not completely understood [19–21]. Segregation may appear in particle species with different material properties, such as size [22], density [23], and restitution coefficient [24].

Size segregation is known as the Brazilian nut (BN) effect when large particles rise to the top; by contrast, in the reverse effect, called the reverse BN (RBN) effect, large particles sink to the bottom. Percolation [25] and convection [26] are representative mechanisms used to explain size separation. Williams [27] first reported percolation, which explains that small particles descend to voids created by the upward movement of large particles. Knight *et al.* [9] studied experimentally the convection mechanism and reported that large particles are transported upward by convection and trapped at the top. At this point, the particles cannot be brought down by the thin downward stream of the convective flow. Notably, only mild convection rates result in size separation because strong convections can enhance mixing [28].

The density segregation of binary mixtures has been a subject of research. Some studies found that the binary mixture separates along the vertical direction. Breu *et al.* [29] experimented with a variety of granular materials to study the transition from the BN effect to the RBN effect. Burtally [30] and Biswas *et al.* [31] investigated equal-size glass-copper systems and found that heavy copper powder rises to the bed top, whereas light glass powder sinks to the bed bottom at low vibration frequencies. However, at high vibration frequencies, the mixture separates into the sandwich configuration, with copper powders distributed at the middle of the bed, in which interstitial gas among the particles plays a decisive role. Shi *et al.* [32] found that light particles tend to rise and form a pure layer at the top of the granular bed, with a mixture of heavy particles and some light particles at the bottom of the bed; these particles form a partially segregated state. Through molecular dynamics simulation, Lim [33] showed that lighter particles tend to rise to the top of the granular bed and form a layer above the heavy particles. Besides BN, RBN, and sandwich segregation, several studies reported that clusters can form in the granular bed [16,23,34–36]. Yang [23] indicated that two convection cells exist in a vibrated system and heavy particles concentrate near the cell centers. According to the simulation performed by Majid and Walzel [36], vibration parameters and container geometries significantly influence convection. Hsiau and Chen [34] investigated the effect of container geometry on density segregation. At the low filling layers, heavier particles migrate to the bottom of the bed. For the high filling layers, the bulk convection motion is the main mechanism that affects segregation; in this case, heavier particles accumulate in the convection center.

This paper studies density segregation under vertical vibration. An equal-size binary mixture of 13X molecular sieve (13XMS) and glass particles is tested in three-dimensional (3D) vibration cylinders. Heavy glass particles cluster as two types, namely, center-type and ring-type cores, under different vibration conditions. The density concentration is also analyzed along the cylinder radius and height. A granular transport model is then established based on heavy-particle movements to study particle distribution and determine the physical relation between convection and segregation.

II. EXPERIMENTAL SETTINGS

A schematic illustration of the proposed experimental system is presented in Fig. 1: A 20-cm-high plexiglass cylindrical container (inner diameter $D = 100$ mm) is fixed on the platform and receives the excitation of vertical vibration from below. A Brüel & Kjær standard vibrating system

*Corresponding author: pingwu@sas.ustb.edu.cn

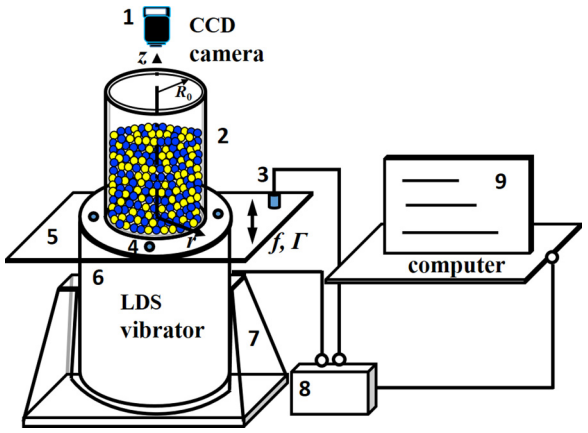

FIG. 1. Schematic presentation of the device: 1, CCD camera; 2, cylindrical container and corresponding cylindrical coordinate system; 3, feedback probe; 4, fixing bolt; 5, horizontal balance plate fixed above the vibrator; 6, standard LDS vibration apparatus; 7, fixed base on the plane floor; 8, switching device; and 9, control systems on the computer.

(instrumental model No. LDS-PDA1000L) is applied to generate sinusoidal vibration in the form of $z = A\sin(2\pi ft)$, where A and f are the vibration amplitude and frequency, respectively. The vibration parameters are modified using terminal software of a personal computer connected to the apparatus. A charge-coupled-device (CCD) camera is fixed above the cylinder to record particle motion on the top free surface. The binary particle mixture is composed of spherical 13XMS and glass particles with the same diameters, dyed yellow and blue, respectively. The physical properties of the two kinds of particles are listed in Table I. The bulk density ρ_b is the ratio of the total mass of single-particle piles to the volume that these particles occupy, including the voids. The filling ratio Φ is the ratio of the material density to the bulk density of the same kind of particle.

We test the binary particle system in the 3D cylindrical container, which is exposed to vertical vibration from below. The vibration parameters are as follows: f varies from 20 to 80 Hz with 2-Hz intervals, whereas Γ varies from 2.0 to 4.0 at 0.2 intervals. The granular mixture finally reaches the steady state and is unaffected by the initial packing of the mixture. The system exhibits a stable distribution after the vibration starts for 50 s.

When the system reaches the steady state, we record particle motion from the top side of the free surface of the particle mixture using a CCD camera (Fig. 1). Based on the continuous images from the 200 frames/s CCD recordings, we observe the motions of the two kinds of particles on the top free surface. Furthermore, we investigate the inner distributions of the two kinds of particles in the steady state in the 3D cylinder. To achieve this goal, we select particles by carefully using a tiny scoop and tweezers in every layer of about the height of the particle diameter along the z axis. We obtain photographs of each cross section and group the two kinds of particles for separate weight measurements as described previously [13].

III. EXPERIMENTAL RESULTS

A. Convection and segregation

We randomly mix 300 g of glass particles and 200 g of 13XMS particles and then place the mixture in a 10-cm-diam cylinder. We then vibrate the particle mixture at $f = 25$ and $\Gamma = 4.0$, where Γ is the dimensionless acceleration amplitude $\Gamma = A(2\pi f)^2/g$, with g the gravity acceleration. Figures 2(a) and 2(c) show the top surface and the side of the bed, respectively. Particles move upward on one side of the container wall [Fig. 2(c)] to the top free surface and the bulk particle flow transfers to the other side [Fig. 2(a)]. The particles move downward along the opposite side [Fig. 2(c)]. This process is designated wall-roll convection. This kind of convection with an inclined surface was also observed in a 2D container by Evesque and Rajchenbach [37]. The inner distributions of the two kinds of particles are also assessed in each divided horizontal cross section. Schematic views of the vertical divisions are shown in Fig. 2(e). The vertical layers are labeled z_1–z_{14} from the bottom to the top and the particle distribution on each vertical layer is shown in Fig. 2(f). Heavy particles (in blue) cluster at the center of the lighter particles (in yellow) on the upper parts of the division views, particularly from z_4 to z_{12}. Figure 2(h) provides a schematic vertical sectional view when wall-roll convection appears. The 13XMS particles are distributed mainly on the bottom and on the layer adjacent to the sidewall as well as on the top free surface, whereas glass particles are mainly distributed at the center of the mixture. We label the two sides of the cylinder outside wall sides A and B, respectively, according to the inclined direction of the slope. The 13XMS particles move upward from the bottom of side A to the top free surface, bounce along the slope, and shift downward to the bottom of side B, forming a circulation. Glass particles possess a larger material density and their motions are slow and confined inside the convection flow of 13XMS particles. Therefore, the cross sections exhibit a center-type core of glass particles [Fig. 2(f)].

Figures 2(b) and 2(d) show the top surface and the side of the bed at $f = 70$ Hz and $\Gamma = 4.0$, respectively. Particles rise from the center of the top free surface and then flow to the periphery [Fig. 2(b)]. Once the particles reach the sidewall, they move downward along the lateral walls [Fig. 2(d)]. This process is referred to as center-roll convection. Heavy particles cluster in the shape of a ring near the sidewall on each layer [Fig. 2(g)]. Figure 2(i) displays a schematic vertical sectional view of center-roll convection. The 13XMS particles move upward from the axial center of the cylindrical container, then

TABLE I. Physical properties of the two kinds of particles selected in our experiment.

Material	Diameter d (mm)	Material density ρ_m (g/cm^3)	Bulk density ρ_b (g/cm^3)	Filling ratio Φ
13XMS	8.00 ± 0.10	0.75 ± 0.05	0.42 ± 0.05	0.56 ± 0.10
glass	8.00 ± 0.05	3.06 ± 0.05	1.71 ± 0.05	0.56 ± 0.05

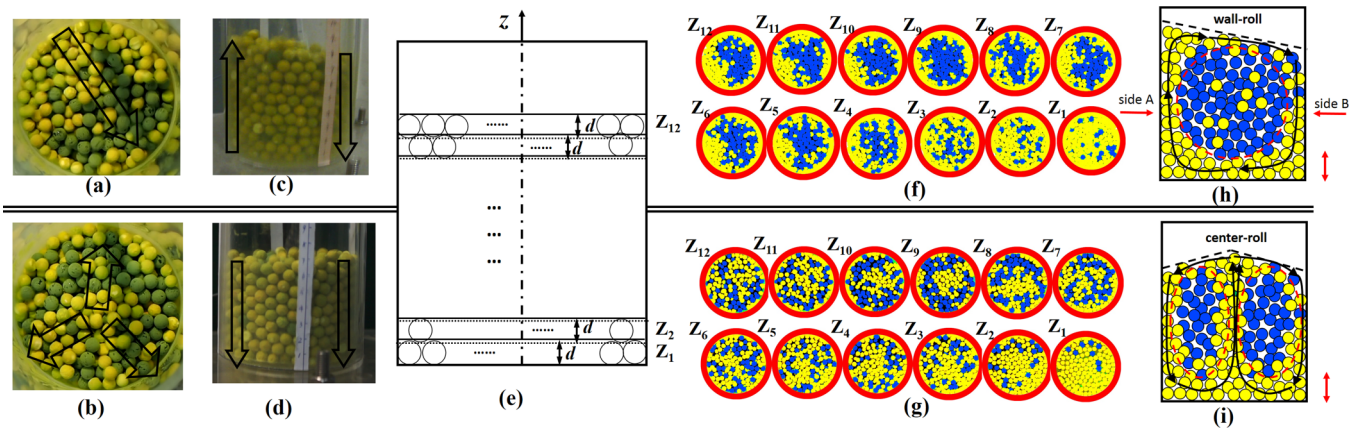

FIG. 2. (a) and (b) Particle movements on the top free surface. (c) and (d) Particle movements on the sidewalls. (e) Schematic views of the vertical divisions. (f) and (g) Distributions of particles on each cross section, with13XMS particles in yellow and glass particles in blue. (h) and (i) Schematic views of the vertical section under two types of convection. The black arrow shows the moving direction of 13XMS particles. The vibration conditions are (a), (c), (f), and (h) $f = 25$ and $\Gamma = 4.0$ and (b), (d), (g), and (i) $f = 70$ and $\Gamma = 4.0$.

bound down along the heap to the sidewall, and slowly relocate downward along the sidewall. Afterward, the particles join the upstream flow at the bottom, forming center-roll convection. Glass particles slowly cluster in the form of the ring-type core, as shown in the cross section [Fig. 2(g)].

The distribution of particles in the steady state is linked with the convection mode; heavy particles (glass particles) tend to cluster and are wrapped inside the flow of the light particles (13XMS particles). We designate the cluster of heavy particles inside the light-particle convection flow a granular core. The granular core phenomenon can also be noted at different inner diameters (80, 100, and 120 mm) of the cylinder container. Furthermore, the granular core phenomenon can be observed for various initial filling heights of the two kinds of particles. In this article we focus on the mixture of 200 g of 13XMS particles and 300 g of glass particles in containers with an inner diameter of 100 mm.

Granular convection varies with changes in vibration parameters (Γ and f). Accordingly, particle segregation and mixing also change, as shown in the phase diagram in Fig. 3. Particle convection and segregation are mainly influenced by the vibration frequency f and are slightly affected by changes in Γ (Fig. 3). At low vibration frequencies ($f < f_1$, A1), the two kinds of particles are both fluidized and the binary particle system tends to mix. At high frequencies ($f > f_4$, A3), the two kinds of particles almost vibrate upward and downward together and their relative positions remain constant. The binary particle system shows a similar solid state. When $f_1 < f < f_2$, the particle mixtures exhibit wall-roll convection (B) and separate as a center-type core [Figs. 2(a), 2(c), 2(f), and 2(h)]. When $f_3 < f < f_4$, the particle mixtures show center-roll convection (C) and separate as a ring-type core [Figs. 2(b), 2(d), 2(g), and 2(i)]. When $f_2 < f < f_3$, the convection mode changes from wall-roll convection to center-roll (A2) convection and the two kinds of particles tend to mix.

B. Particle distribution

Particle distribution is studied to understand the granular core phenomenon with the two different types of segregation. We fix $\Gamma = 4.0$ and only vary the vibration frequency f because the effect of Γ is not significant. When $20\,\text{Hz} < f < 40\,\text{Hz}$, wall-roll convection appears with a center-type cluster of glass particles. At $50\,\text{Hz} < f < 70\,\text{Hz}$, center-roll convection and a ring-type cluster of glass particles are obtained.

When the system reaches the steady state, we stop the vibration. Particles in every divided vertical layer [$z_1 - z_{12}$ in Fig. 2(c)] are selected by a scoop and tweezers and when we take out the particles on the upper layer, the distribution of the remaining particles is not affected. The masses of the two kinds of particles in each layer are weighed to study vertical distribution. The images of each horizontal cross section of each layer are processed to study the radial distribution of the particles. For a binary mixture of particles that differ in density, the subscript i denotes each species ($i = H$ represents heavy particles, herein for glass particles, and $i = l$ represents

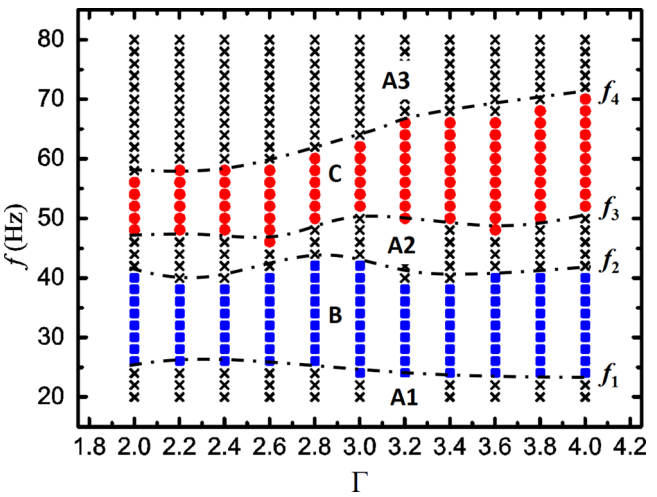

FIG. 3. Phase diagram of particle convection and segregation: ×, mixed state; ■, center-core segregation; ●, ring-core segregation; A1, fluidized system; B, wall-roll convection; A2, transitional state from wall-roll to center-roll convection; C, center-roll convection; and A3, solid state.

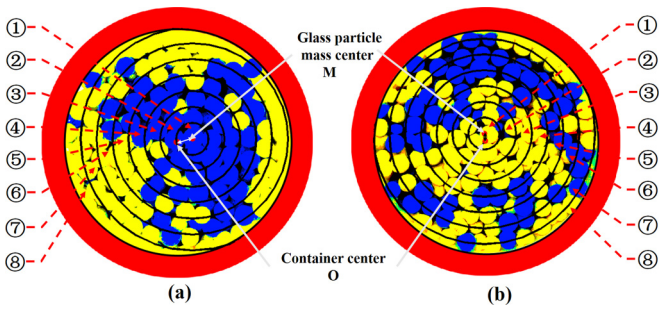

FIG. 4. Radial divisions in the horizontal cross sections for the (a) circle-type and (b) ring-type granular cores. Numbers 1–8 represent the rings from the mass center to the outside wall.

small particles, herein for 13XMS particles). The masses of the two kinds of particles on the jth layer are denoted by $m_{H,j}$ and $m_{L,j}$. The particle sizes of the two kinds of particles are almost the same and their densities are denoted by ρ_H and ρ_L, respectively. Hence, the heavy-particle number concentration in each vertical layer φ_z can be defined as

$$\varphi_z = \frac{\frac{m_{H,j}}{\rho_H}}{\frac{m_{H,j}}{\rho_H} + \frac{m_{L,j}}{\rho_L}}. \quad (1)$$

Afterward, the images of each horizontal section on layers z_1–z_{12} are processed to obtain the radial distributions of heavy particles. The two kinds of particles are differentiated by color (Fig. 4). Heavy particles correspond to glass particles (blue) and light particles correspond to 13XMS particles (yellow). The red ring defines the container margin. The coordinates of the center of the circular cross section are set at $O(0,0)$. All the coordinates of the blue pixels can be recorded as $(x_1,y_1),(x_2,y_2),\ldots,(x_n,y_n)$, where n is the total number of pixels on the layer. Thus, the mass center M_j of heavy particles on the jth layer (X_j,Y_j) can be calculated as follows:

$$X_j = \left(\frac{\sum_{k=1}^{n} x_k}{n}\right)_j, \quad Y_j = \left(\frac{\sum_{k=1}^{n} y_k}{n}\right)_j. \quad (2)$$

Each cross section is divided into eight rings from the mass center of heavy particles to the wall. The distance between two adjacent rings is fixed at 7.3 mm in the 100-mm-diam container. The glass particle mass center deviates from the bed center; hence, waning rings exist near the bed wall (Fig. 4). The pixel numbers of the two kinds of particles in each ring (rings 1–8) are counted. The subscript (i,j) (i = 1,2,3,...,8; j = 1,2,3,...,12) denotes the ith ring on the jth layer. The pixel number in each ring at the vertical layer is labeled $n_{H,(i,j)}$ for heavy particles and $n_{L,(i,j)}$ for light particles. The heavy-particle number fraction can be calculated as

$$\varphi_{(i,j)} = \frac{n_{H,(i,j)}}{n_{H,(i,j)} + n_{L,(i,j)}}. \quad (3)$$

Figure 5(a) shows the particle distributions at $f = 25$ Hz and $\Gamma = 4.0$ for the wall-roll convection, whereas Fig. 5(b) shows those at $f = 70$ Hz and $\Gamma = 4.0$ for center-roll convection. In these cases, $r = 0$ and $z_j = 0$ represent the mass center of heavy particles and the bottom of the bed, respectively. Figures 5(c) and 5(d) indicate the φ_z along the bed height, where $\varphi_z = \sum \varphi_{(i,z)}$, with i = 1–8. The value of φ_z is small and changes in φ along the radius are not constant at layers z_1–z_3. The bottom of the granular bed is dominated by light particles, whereas the heavy particles are widely dispersed. On the upper layers (z_4–z_{12}), φ_z increases. At the top layer of the granular bed (z_{12}), heavy particles are unconfined and

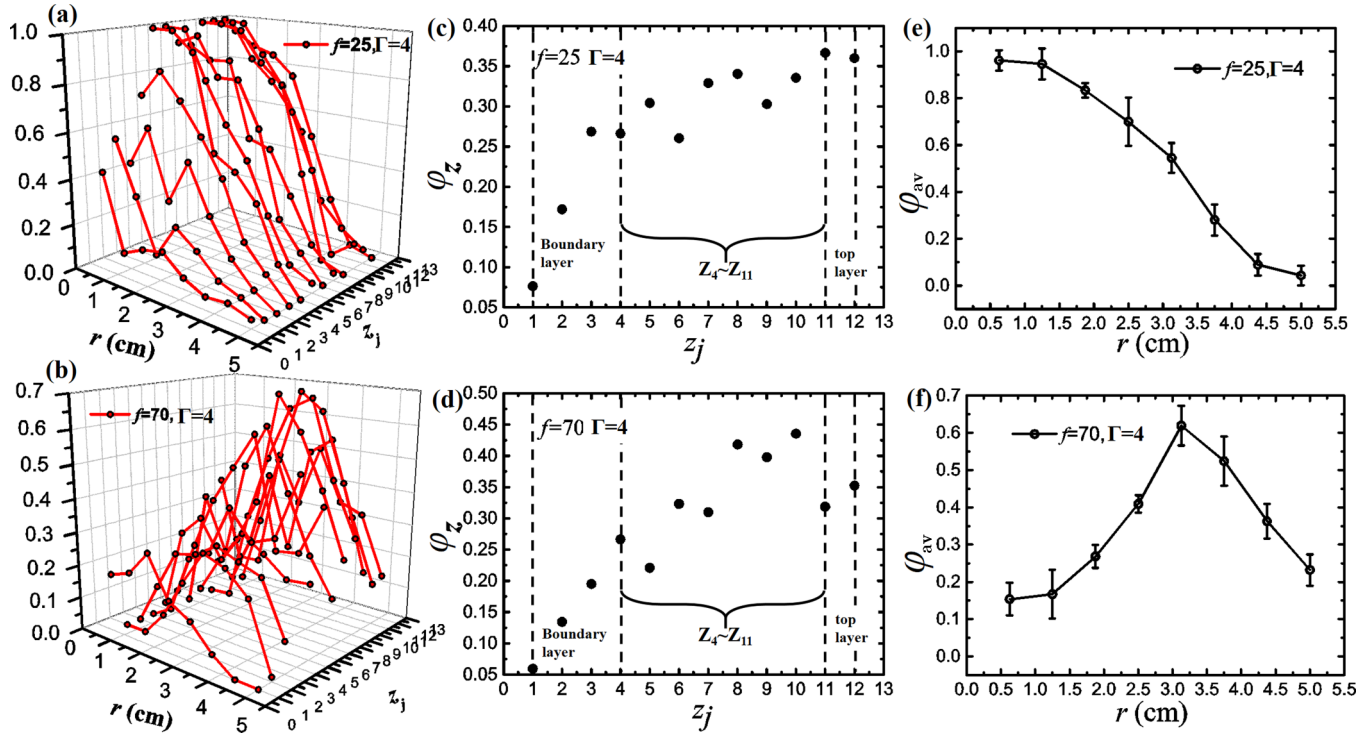

FIG. 5. Heavy-particle distribution for (a), (c), and (e) $f = 25$ Hz and $\Gamma = 4.0$ and (b), (d), and (f) $f = 70$ Hz and $\Gamma = 4.0$.

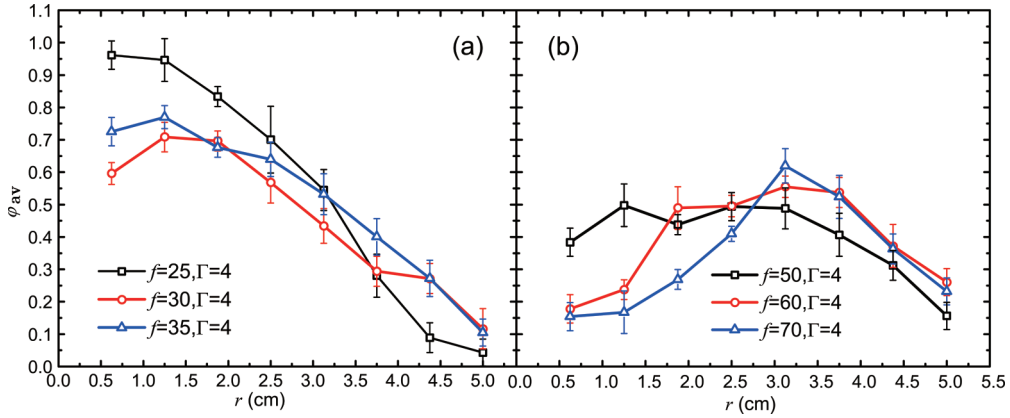

FIG. 6. Plot of φ_{av} versus r under different f.

randomly distributed. At layers z_4−z_{11}, φ along the radial direction shows a regular distribution. Therefore, we average φ from layers z_4−z_{11} to estimate the radial distribution, given that $\varphi_{av} = \sum \varphi_{(i,z)}$ and $z = 4$−11. The averaged radial distribution with its standard error is shown in Figs. 5(e) and 5(f). For the wall-roll convection at $f = 25$ Hz and $\Gamma = 4.0$, φ_{av} decreases from the mass center to the outer walls. This result indicates that heavy particles are distributed mainly at the mass center of the cluster. For the center-roll convection at $f = 70$ Hz and $\Gamma = 4.0$, φ_{av} is small in the mass center, increases to a peak, and then drops at the wall. This finding implies that heavy particles are distributed on a ring around the mass center on each circular cross section.

C. Granular core

In our experiments, the effects of f on the separation patterns are studied and the average radial distribution of glass particles in the two frequency ranges of wall-roll convection and center-roll convection when $\Gamma = 4.0$ in the phase diagram (Fig. 3) is shown in Figs. 6(a) and 6(b). From the curves of the center core of glass particles under wall-roll convection in Fig. 6(a), φ_{av} decreases from the mass center to the wall. In Fig. 6(b) φ_{av} increases to reach the peak in the middle position of r before decreasing at the wall. In the two frequency ranges, there are heavy-particle cores at different positions: In the first condition, the granular core is at the center and in the second condition, the granular core is between the mass center and the wall.

From the curves above we can only know the trend of the particle number density from the heavy-particle mass center to the wall. To quantify the position of the heavy-particle core and show its position in the radial direction, we define Δl_j as the distance between the heavy-particle mass center $M_j(X_j, Y_j)$ at the layer z_j and the bed center $O(0,0)$. The expression for Δl_j is

$$\Delta l_j = \sqrt{X_j^2 + Y_j^2}. \tag{4}$$

In this case, (X_j, Y_j) is the coordinate of M_j. We further define Δl as

$$\Delta l = \frac{1}{8} \sum_{j=4}^{j=11} \Delta l_j \tag{5}$$

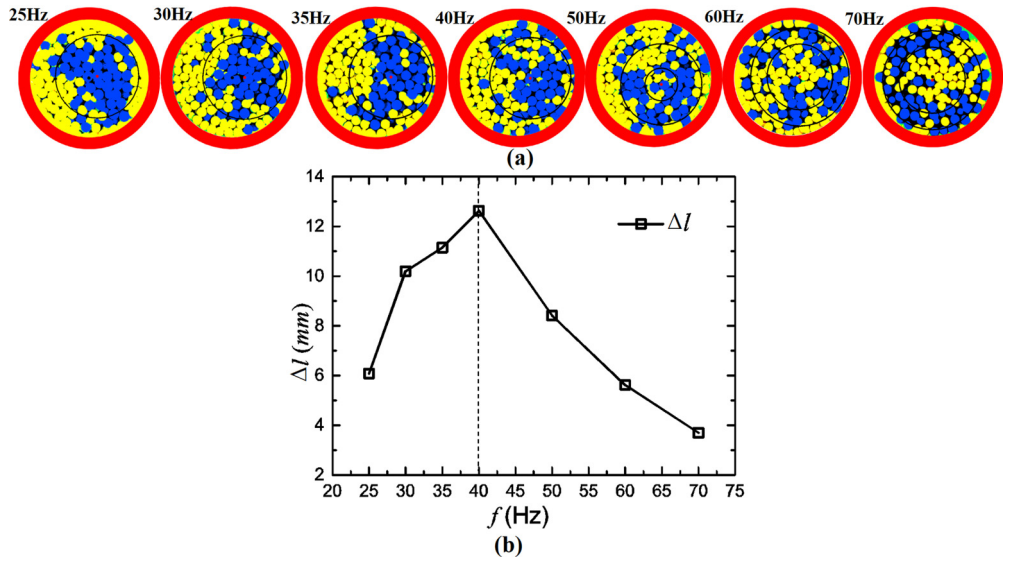

FIG. 7. (a) Cross-sectional views at layer z_{10} under different f. The plot at 25–40 Hz shows the circle-type core of glass particles, whereas that at 50–70 Hz shows the ring-type core. (b) Curves of Δl under different frequencies.

to estimate the deviation of the granular core to the container bed center because Δl_j changes with layer position. If Δl equals zero, the mass center of the granular core is located at the container central axis. From the cross-sectional views in Fig. 7(a) as well as the curve of Δl for different f, we can find that for the two types of granular cores, when $f =$ 25 and 70 Hz, the heavy particles are distributed relatively symmertrically in the cross sections and in other cases the granualar core center deviates more significantly from the axis center.

IV. PHYSICAL MODEL

When there are only 13XMS particles in the granular bed, these particles form the same convection patterns as the binary particles mixtures in the two frequency ranges [Figs. 8(a) and 8(b)]. After the heavy particles are added into the mixture they join the upflow of the light particles and then reach the top free surface. Once the heavy particles are carried down along the wall, as shown in Fig. 8(c), they are supported by light particles from below as well as by the pressure from the flux of light particles from the top surface down along the wall. The outer layer of particles is more compact than the inner layer, which can be traced from the experimental studies of packing fraction by Wildman *et al.* [38], which reported a sudden increase in the packing fraction near the wall. In addition, the velocity of heavy particles is much smaller than that of the light ones. After the collision between neighboring particles, the direction of the resultant forces on the heavy particles points to the inner looser layer, so the heavy particles are squeezed from the outer layer, then move into the loosely packed region, taking the place of the light particles there, and then are constrained by the light-particle flow. So when the system reaches the steady state, the heavy particles mainly distribute in the inner circle of the convection flow. In the z axis direction, the heavy particles flow in the direction of convection. In the r direction, there is particle exchange in this direction, as shown in Figs. 8(d)–8(f), and heavy particles in the inner cluster particle will go to the outer layer due to the movement imposed on them and at the same time heavy particles in the outer layer will also be squeezed inside. To

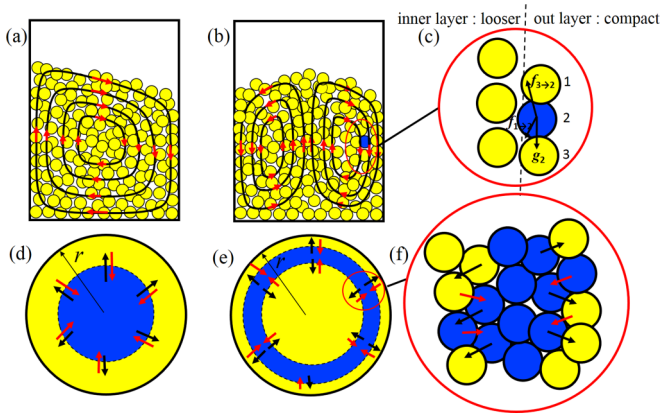

FIG. 8. Particle convection pattern in (a) and (b) the single-particle system, (c) the force of heavy particles added into the system, and (d)–(f) the cross-sectional views of radial exchange of heavy particles under steady state.

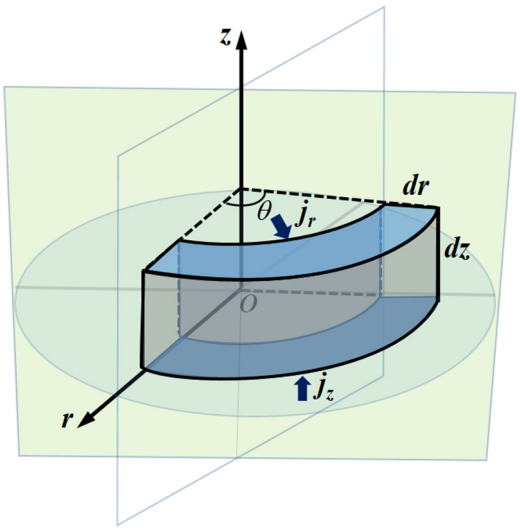

FIG. 9. Sketch of the controlled volume for j_r and j_z under the polar coordinate system in the cylindrical container.

describe the exchange of heavy particles in the radial direction in the steady state, we apply a form similar to diffusion, which is the result of the integrated effect of heavy-particle movement in the radial direction.

We note that heavy particles clustered in the bed are closely linked with convection modes, which are affected by vibration conditions. In our experiment, we mainly investigate the effect of f. The particle transport model is set up with heavy particles as the object. The transport equations are then solved when the granular bed reaches the steady state.

From the experiment results we know that the convection mode varies for different f, which was also reported in former experiments in the 2D granular bed [12]. To simplify the physical model, supposing the convection roll is symmetric, for the first condition of convection, the center of convection roll is the axial center and for the second condition of convection roll, the convection is symmetric along the radial direction. According to the assumption, the particle flow is in the radial and vertical directions j_r and j_z, respectively, as shown in the cylindrical controlled volume in Fig. 9. Given this mass conservation, the transport of equations in the steady state can be described as

$$\frac{1}{r}\frac{\partial}{\partial r}(r j_r) + \frac{\partial}{\partial z}(j_z) = 0. \tag{6}$$

When the system reaches the steady state, the flow of heavy particles in the vertical direction is carried by light particles. The expression for j_z can be written as $j_z = u_z\varphi$, where u_z is the vertical velocity of particles in the granular bed. The experimental results of Knight *et al.* [9] demonstrated the exponential decrease of u_z from the top free surface into the granular bed, and the radial dependence of the velocity can be approximated by either a hyperbolic cosine function or modified zeroth-order Bessel functions. In our experiment, we suppose the expression of u_z as

$$u_z = C_z(s^2 - r^2), \tag{7}$$

where $C_z = e^{mz}(m > 0)$; r and z are the particles' coordinates along the radius and height, respectively; m is the parameter

influenced by particle convection; and s is the radius position at $u_z = 0$. Moreover, $0 \leqslant s < R_0$, where R_0 is the radius of the bed. When $s = 0$, the velocity profile corresponds to wall-roll convection; when $r = 0$, $u_z = 0$. The expression (11) is similar to that proposed by Knight *et al.* [9] when $0 < s < R_0$, because the granular bed shows a center-roll convection. The upward velocity changes in the radial direction. At the radial position where $r = s$, u_z is zero. At $0 < r < s$, $u_z > 0$ and the particles rise from the bed bottom to the top. At $s < r < R_0$, $u_z < 0$ and the particles sink. When $s = 0$, no particle flow is observed at the center ($r = 0$), because $u_z = 0$. When $0 < r < R_0$, the direction of the flow is a single-roll convection on one side of the container. Therefore, u_z can obtain two convection modes by changing s, in particular, wall-roll and center-roll convections.

The flow of heavy particles in the vertical direction in the steady state is induced by convection in the granular bed. The particles perform a random walk along the radial direction because of random collisions, as observed from the sidewall (some particles move inside, whereas some exit after the collision). This process in the radial direction caused by velocity fluctuations can be described in the form of diffusion as $j_r = -D_r \partial\varphi/\partial r$, where D_r is the diffusion coefficient. In dense granular systems of monodisperse or bidisperse particles differing only in density, the diffusion coefficient D_r scales as γd^2, where γ is the share rate and d is the particle diameter [6,39,40]. Fan *et al.* [41] reported that D_r scales as γd^2 only at high shear rates. However, when the shear rate is below the critical value, the coefficient D_r is independent of γd^2. In our study the diffusion in the radial direction is induced by shear generated by convection flow. Under the vibration condition (f, Γ), the shear rate is small; thus we simplify the diffusion coefficient D_r and set the variable as constant.

According to the supposition and analysis above, the expressions of j_r and j_z show the relationship between particle flow and heavy-particle number concentration. By substituting the expressions in the transport equation, we achieve the heavy-particle number concentrations.

The transport equation is therefore given by

$$-\frac{1}{r}\frac{\partial}{\partial r}\left(r D_r \frac{\partial\varphi}{\partial r}\right) + \frac{\partial}{\partial z}(u_z\varphi) = 0. \tag{8}$$

The boundary conditions for the two types of granular core distribution are the same: Both have to be fitted in the mass conservation of the system. The integral of φ with respect to r equals φ_z. Furthermore, the integral of φ_z with z refers to the total amount of heavy particles with respect to all particle amounts in the granular bed:

$$\frac{\int_0^{R_0}\varphi\, r dr}{\int_0^{R_0} r dr} = \varphi_z, \quad \int_0^{z_{12}} \varphi_z dr = C_\varphi \int_0^{z_{12}} dr, \tag{9}$$

where C_φ is the volume fraction of heavy particles in the granular bed. To get the specific solution to the equation corresponding to the experimental conditions, for the ring-type core, we give the heavy-particle number fraction at the wall for a different height $\varphi_{(r=R_0)} = f(z)$.

By using the separation variables $\varphi(r,z) = R(r)H(z)$, we define expression (8) as

$$\frac{1}{r}D_r H R' + D_r H R'' - (s^2 - r^2)R\left(\frac{\partial C_z}{\partial z}H + C_z H'\right) = 0, \tag{10}$$

$$\frac{rR' + r^2R''}{r^2(s^2 - r^2)R} = \frac{\frac{\partial C_z}{\partial z}H + C_z H'}{H D_r} = k, \tag{11}$$

where k is the proportional coefficient and the separated functions for R give

$$r^2R'' + rR' + kr^2(r^2 - s^2)R = 0. \tag{12}$$

The heavy-particle concentration is always finite in the cylinder, thus the value of k should be above zero. We let $k = \lambda^4 > 0$. For the wall-roll condition, $s = 0$ and the solution for Eq. (12), where $r^2R'' + r^2R' + \lambda^4 r^4 R = 0$, is

$$R = J_0\left(\tfrac{1}{2}(\lambda r)^2\right). \tag{13}$$

For the ring-roll convection, $s \neq 0$ and the solution for Eq. (16), where $r^2R'' + r^2R' + \lambda^4 r^2(r^2 - s^2)R = 0$, can be described using the power series $R = \Sigma_{n=0}^{\infty} a_n x^n$, where $x = \frac{1}{2}(\lambda r)^2$. We give the first three terms of R by substituting the power series in the partial equation as follows:

$$R = a_0 + q a_0 \frac{1}{2}(\lambda r)^2 + \frac{q^2 a_0^2 - a_0}{4}\frac{1}{4}(\lambda r)^4 + \frac{q^3 a_0^2 - 5q a_0}{36}\frac{1}{8}(\lambda r)^6, \tag{14}$$

where $q = (\lambda s)^2/2$.

The separated function for H can be rewritten as

$$\frac{\partial C_z}{\partial z} + \frac{C_z H'}{H} = k D_r. \tag{15}$$

By substituting the expression $C_z = e^{mz}$ in Eq. (15), we solved the equation as

$$H = \exp\left(\frac{k D_r}{m}e^{-mz} - mz\right). \tag{16}$$

The solution to Eq. (12) for the wall-roll convection can therefore be described as

$$\varphi(r,z) = \sum_{n=1}^{\infty} A_n J_0\left(\frac{1}{2}(\lambda_n r)^2\right)\exp\left(-\frac{\lambda_n^4 D_r}{m}e^{-mz} - mz\right). \tag{17}$$

To simplify expression (17), we used the first term of the series as approximate value:

$$\varphi(r,z) = A_1 J_0\left(\frac{1}{2}(\lambda_1 r)^2\right)\exp\left(-\frac{\lambda_1^4 D_r}{m}e^{-mz} - mz\right). \tag{18}$$

The expression of φ for the center-roll condition can be given as

$$\varphi(r,z) = A_1\left(a_0 + q a_0 \frac{1}{2}(\lambda r)^2 + \frac{q^2 a_0^2 - a_0}{4}\frac{1}{4}(\lambda r)^4 + \frac{q^3 a_0^2 - 5q a_0}{36}\frac{1}{8}(\lambda r)^6\right)\exp\left(-\frac{\lambda^4 D_r}{m}e^{-mz} - mz\right). \tag{19}$$

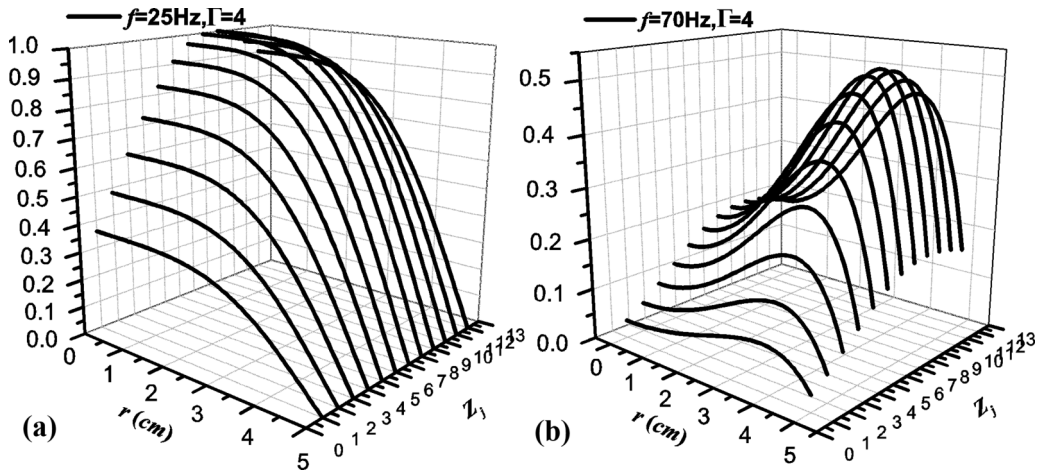

FIG. 10. Theoretical data of φ plotted against r under vertical layers z_j for (a) $f = 25$ Hz and $\Gamma = 4$ and (b) $f = 70$ Hz and $\Gamma = 4$.

The theoretical curves of φ under the two granular core conditions are plotted in Figs. 10(a) and 10(b). The experimental results of 25 and 70 Hz in the two convection modes are relatively symmetric in the granular bed. Results from the solution of the physical model agree in Figs. 10(a) and 10(b) with the experimental results in Figs. 5(a) and 5(b). Heavy particles are mainly distributed on the upper part of the granular bed. For the center-type core under wall-roll convection when $f = 25$ Hz, heavy particles dominate the center of the circular section and drop to almost zero at the sidewall. For the ring-type core under the center-roll condition, the heavy-particle concentration reaches a maximum at $r = 3.7$ cm under each vertical layer. The center of the circular section and the sidewalls is dominated by light particles.

According to expression (18) and the condition of φ_z in expressions (9), the theoretical φ_z under wall-roll convection can be described as

$$\varphi_z = \frac{\int_0^{R_0} \varphi\, r dr}{\int_0^{R_0} r dr} = \frac{\int_0^{R_0} A_1 J_0\left(\frac{1}{2}(\lambda_1 r)^2\right) \exp\left(-\frac{\lambda_1^4 D_r}{m} e^{-mz} - mz\right) r dr}{\int_0^{R_0} r dr} = B_1 \exp\left(-\frac{\lambda_1^4 D_r}{m} e^{-mz} - mz\right), \tag{20}$$

where B_1 is the coefficient determined by the integral of $R(r)$. To compare the theoretical φ_{av} from layers $z_j = 4{-}11$ with the experimental data, we calculate φ_{av} as

$$\varphi_{\text{av}} = \frac{1}{8}\sum_{z=4}^{z=11} \varphi = \frac{1}{8}\sum_{z=4}^{z=11} A_1 J_0\left(\frac{1}{2}(\lambda_1 r)^2\right) \exp\left(-\frac{\lambda_1^4 D_r}{m} e^{-mz} - mz\right) = C_1 J_0\left(\frac{1}{2}(\lambda_1 r)^2\right), \tag{21}$$

where C_1 is a function of D_r and m. Similarly, the expressions of φ_z and φ_{av} for the center-roll convection can be expressed as

$$\varphi_z = B_1 \exp\left(-\frac{\lambda_1^4 D_r}{m} e^{-mz} - mz\right), \tag{22}$$

$$\varphi_{\text{av}} = C_1\left(a_0 + q a_0 \frac{1}{2}(\lambda r)^2 + \frac{q^2 a_0^2 - a_0}{4}\frac{1}{4}(\lambda r)^4 + \frac{q^3 a_0^2 - 5 q a_0}{36}\frac{1}{8}(\lambda r)^6\right), \tag{23}$$

where φ_z should fit Eq. (9) and $C_\varphi = 0.272$ for the binary mixture of 300 g of glass particles and 200 g of 13XMS particles. The φ_z with the function of z for different frequencies ($f = 25$ and 70 Hz) are plotted in Fig. 11(a). The shape of the curves remain the same. The two curves also show that more heavy particles are distributed on the upper part of the granular bed when f increases. This result agrees with previous findings [13]. When f increases, the energy imported into the bed E decreases in accordance with the relationship between the energy and the vibration conditions in the studies of Xie *et al.* [2], where $E \approx \Gamma^2/f^2$. In such a relation, energy is inversely proportional to the square of f. The energy imported into the bed decreases with increasing f. The convection intensity decreases because of the decrease in imported energy. More heavy particles are also trapped in the upper part of the granular bed. The radial trends of φ_{av} for different f are different for the two convection modes [Figs. 11(b)]. The convection in the vertical direction is assumed to be $u_z = C_z(s^2 - r^2)$. For the wall-roll convection, $s = 0$ and the value of φ_{av} reaches its peak at $r = 0$ from the theoretical solutions; at this position the vertical velocity equals zero and the concentration of the heavy particle is almost zero at the sidewall. For the center-roll convection, $s \neq 0$ and the curve of φ_{av} reaches its peak around $r = 3.7$ cm; the position where $u_z = 0$ is $r = 4.0$ for the 70-Hz condition. By comparing the two convection modes, we find that the

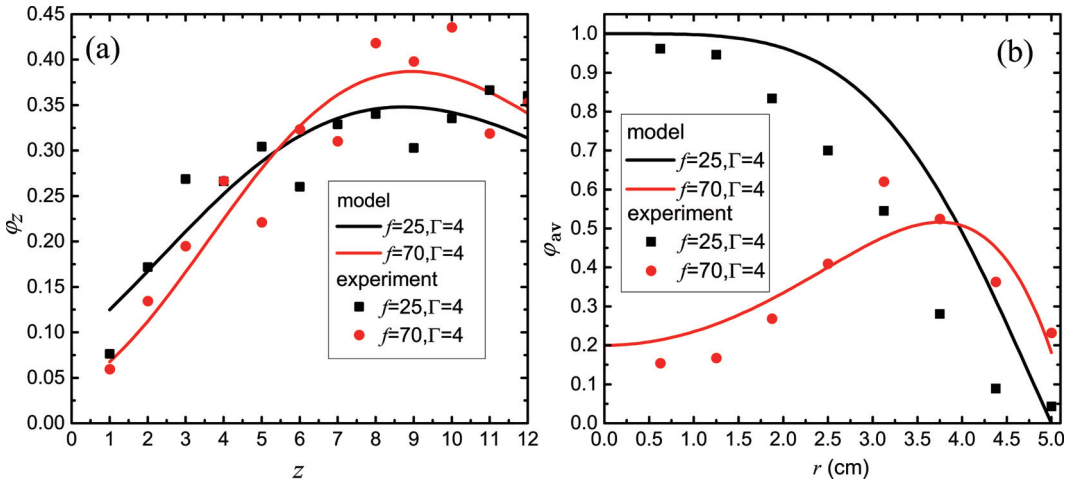

FIG. 11. Theoretical curves and experimental data of φ_z versus z and φ_{av} versus r when $f = 25$ and 70 Hz.

position of the heavy-particle core in the radial direction is linked with the convection velocity field, whereas the diffusion in the radial direction affects the clustering extent. The heavy particles tended to cluster in the radial range where the vertical velocity is small.

V. CONCLUSION

By vertically vibrating equal-size granular mixtures in cylinders, heavy particles can cluster and exhibit two types of clustering for vibration parameters. The vibration frequency f strongly influenced particle convection and particle cluster modes, whereas the dimensionless acceleration amplitude Γ only showed minimal effects. At $\Gamma = 4.0$ in our experiments, the particle mixtures showed a wall-roll convection and heavy particles clustered as a center-type core at $20\,\text{Hz} < f < 40\,\text{Hz}$. With increasing f, the deviation of the center-type core center and the bed center increased and the core moved to the bed wall. The particle mixtures displayed a center-roll convection and separated as a ring-type core at $50\,\text{Hz} < f < 70\,\text{Hz}$. With increasing f, heavy particles were separated completely and the center of the ring-type core gradually shifted to the center of the bed. The heavy-particle distribution was found to be closely linked with convection modes and the velocity field in the granular bed. Given the symmetric condition of the physical model, we compared the results of 25 and 70 Hz in experiments. The heavy-particle distribution along the bed height satisfied the exponential functions under center-type and ring-type cores. However, the heavy-particle distribution in the radial direction of the two types of clusters differed. For the ring-type core, the radial distribution followed the first-order Bessel function of the first kind, whereas for the center-type core, the radial distribution was simplified using the first three terms of the power series.

VI. ACKNOWLEDGMENTS

The authors are grateful for support from the National Natural Science Foundation of China (Grants No. 51476009 and No. 51506006) and the Fundamental Research Funds for the Central Universities (Grant No. FRF-SD-15-018A3).

[1] Z. Xie, P. Wu, S. Wang, Y. Huang, S. Zhang, S. Chen, C. Jia, C. Liu, and L. Wang, Soft Matter **9**, 5074 (2013).
[2] Z.-A. Xie, P. Wu, S.-P. Zhang, S. Chen, C. Jia, C.-P. Liu, and L. Wang, Phys. Rev. E **85**, 061302 (2012).
[3] N. Shishodia and C. R. Wassgren, Phys. Rev. Lett. **87**, 084302 (2001).
[4] D. A. Huerta and J. C. Ruiz-Suárez, Phys. Rev. Lett. **92**, 114301 (2004).
[5] G. G. Pereira, N. Tran, and P. W. Cleary, Granular Matter **16**, 711 (2014).
[6] A. Tripathi and D. V. Khakhar, J. Fluid Mech. **717**, 643 (2013).
[7] M. Faraday, Philos. Trans. R. Soc. London **121**, 299 (1831).
[8] S. Hsiau and C. Chen, Powder Technol. **111**, 210 (2000).
[9] J. B. Knight, E. E. Ehrichs, V. Y. Kuperman, J. K. Flint, H. M. Jaeger, and S. R. Nagel, Phys. Rev. E **54**, 5726 (1996).
[10] Y.-h. Taguchi, Phys. Rev. Lett. **69**, 1367 (1992).
[11] Y. Lan and A. D. Rosato, Phys. Fluids **9**, 3615 (1997).
[12] F. Zhang, L. Wang, C. Liu, P. Wu, and S. Zhan, Phys. Lett. A **378**, 1303 (2014).
[13] K. Hu, Z. A. Xie, P. Wu, J. Sun, L. Li, C. Jia, S. Zhang, C. Liu, and L. Wang, Soft Matter **10**, 4348 (2014).
[14] D. A. Sanders, M. R. Swift, R. M. Bowley, and P. J. King, Phys. Rev. Lett. **93**, 208002 (2004).
[15] B. Meerson, T. Pöschel, and Y. Bromberg, Phys. Rev. Lett. **91**, 024301 (2003).
[16] N. Rivas, S. Ponce, B. Gallet, D. Risso, R. Soto, P. Cordero, and N. Mujica, Phys. Rev. Lett. **106**, 088001 (2011).
[17] H. M. Jaeger, S. R. Nagel, and R. P. Behringer, Rev. Mod. Phys. **68**, 1259 (1996).
[18] Z.-A. Xie *et al.*, Powder Technol. **260**, 1 (2014).
[19] X. Yan, Q. Shi, M. Hou, K. Lu, and C. K. Chan, Phys. Rev. Lett. **91**, 014302 (2003).

[20] L. Trujillo, M. Alam, and H. J. Herrmann, Europhys. Lett. **64**, 190 (2003).
[21] J. Talbot and P. Viot, Phys. Rev. Lett. **89**, 064301 (2002).
[22] K. Ahmad and I. J. Smalley, Powder Technol. **8**, 69 (1973).
[23] S. C. Yang, Powder Technol. **164**, 65 (2006).
[24] R. Brito and R. Soto, Eur. Phys. J. Spec. Top. **179**, 207 (2009).
[25] A. Rosato, K. J. Strandburg, F. Prinz, and R. H. Swendsen, Phys. Rev. Lett. **58**, 1038 (1987).
[26] S. S. Hsiau, P. C. Wang, and C. H. Tai, AlChE J. **48**, 1430 (2002).
[27] J. C. Williams, Powder Technol. **15**, 245 (1976).
[28] D. Brone and F. J. Muzzio, Phys. Rev. E **56**, 1059 (1997).
[29] A. P. J. Breu, H. M. Ensner, C. A. Kruelle, and I. Rehberg, Phys. Rev. Lett. **90**, 014302 (2003).
[30] N. Burtally, Science **295**, 1877 (2002).
[31] P. Biswas, P. Sánchez, M. R. Swift, and P. J. King, Phys. Rev. E **68**, 050301 (2003).
[32] Q. Shi, G. Sun, M. Hou, and K. Lu, Phys. Rev. E **75**, 061302 (2007).
[33] E. W. C. Lim, AlChE J. **56**, 2588 (2010).
[34] S.-S. Hsiau and W.-C. Chen, Adv. Powder Technol. **13**, 301 (2002).
[35] D. Paolotti, C. Cattuto, U. M. B. Marconi, and A. Puglisi, Granular Matter **5**, 75 (2003).
[36] M. Majid and P. Walzel, Powder Technol. **192**, 311 (2009).
[37] P. Evesque and J. Rajchenbach, Phys. Rev. Lett. **62**, 44 (1989).
[38] R. D. Wildman, J. M. Huntley, and D. J. Parker, Phys. Rev. E **63**, 061311 (2001).
[39] B. Utter and R. P. Behringer, Phys. Rev. E **69**, 031308 (2004).
[40] Y. Fan, C. P. Schlick, P. B. Umbanhowar, J. M. Ottino, and R. M. Lueptow, J. Fluid Mech. **741**, 252 (2014).
[41] Y. Fan, P. B. Umbanhowar, J. M. Ottino, and R. M. Lueptow, Phys. Rev. Lett. **115**, 088001 (2015).